SHIP WAVES GENERATED BY A CRUISE SHIP: FIELD OBSERVATION AND NUMERICAL REPRESENTATION USING GREEN'S FUNCTIONS

Yoshimitsu Tajima, The University of Tokyo, yoshitaji@coastal.t.u-tokyo.ac.jp
Jumpei Morioka, Data Analytics Labo Co. Ltd., jumpei.morioka@dalab.jp
Yusuke Yamanaka, Hokkaido University, yyamanaka@sci.hokudai.ac.jp
Björn Almström, Lund University, bjorn.almstrom@tvrl.lth.se
Magnus Larson, Lund University, magnus.larson@tvrl.lth.se

INTRODUCTION

Along fairways, rivers, and sheltered seas, ship waves may have dominant influence on shore and bank erosion and disturb the ecosystem (e.g., Larson et al. 2017, Almström et al., 2022). For efficient and reliable prediction of ship wave generation, the authors developed a numerical model based on Green's functions (Morioka et al., 2020). While reasonably good model performance was confirmed through comparison with measured data in a laboratory experiment, observed ship waves, generated by a relatively small model boat, were dominated by secondary wave components with relatively short periods. Model applicability for prediction of primary wave components, dominantly generated by a large vessel, was not established. Primary waves are induced by the pressure head drop around a vessel, whereas secondary waves are generated through water surface disturbances induced around the bow and the stern. Differences in the physical mechanisms of these two wave components make it difficult for a model to represent both components using a simple unified methodology.

This study presents results from a unique field survey of ship waves generated by a cruise ship along a sheltered coastal fairway in Sweden, including the application and enhancements of the aforementioned model, which improved predictions of both the observed primary and secondary ship wave components.

FIELD SURVEY

The field survey was conducted at Staboudde in the Stockholm Archipelago on the east coast of Sweden (Fig. 1). Staboudde is located at strait and has suffered bank erosion and disturbances due to waves generated by large ships passing. Fig. 2 shows the bathymetry around the field survey site. In the figure, the solid triangle indicates the location where the water surface fluctuations due to ship waves were observed. The time-varying water surface levels were obtained through image analysis in which the instantaneous water level along the vertical pole placed at the target point was extracted. Among several vessels passing during the survey, we selected the ship waves generated by a large cruise ship in which both primary and secondary wave components were clearly observed. The dimensions of this ship were 218 m in length, 31.8 in width, and 6.8 m in maximum draft. The navigation speed of the vessel was around 10 - 17 kn.

Blank circles in Fig. 2 indicate the track of this vessel obtained from AIS. Fig. 3 shows the observed time history of the water surface level at the observation point with water depth of 0.78 m. As seen in the figure, the time profile shows the first primary wave with a period of around 80 sec followed by shorter secondary waves with period of around 2 sec. It was confirmed that the water surface level variation extracted from different poles installed around the observation point were similar.

MODEL APPLICATION

In the present model based on Green's functions, the time-varying water level at an arbitrary location P_j, shown in Fig. 4, is determined by a linear summation of the water level fluctuations at P_j generated from discrete points, Z_i, along the navigation route with a unit wave source specified by a Gaussian pulse. In the linear summation, Gaussian pulse at Z_i is applied when the segment of this ship body, s_k, passes

Figure 1 Location of Staboudde

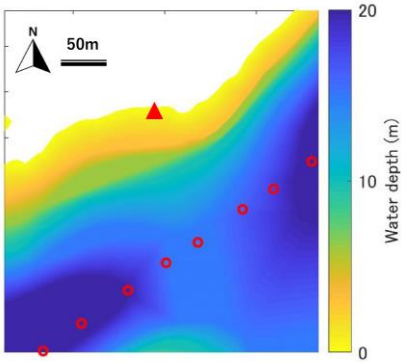

Figure 2 Bathymetry around the field survey site

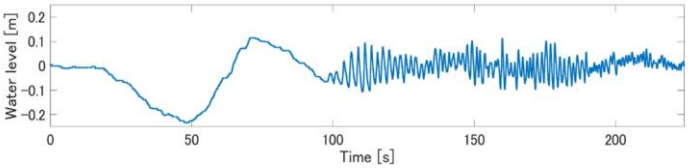

Figure 3 Observed water level fluctuations near the shore with water depth of around 0.78m

Z_i. The magnitude of the Gaussian pulse at each segment, s_k, is determined through linear inversion so that computed water level profile at P_j matches with the observed one.

Although the propagation of the Gaussian pulse from each source point, Z_i, to the target point, P_j, can be computed by a linear dispersive wave model, for example the linear Boussinesq equations (e.g., Nwogu, 1993), these equations may have a problem to accurately describe the wave dispersion relationships of high frequency waves relative to the water depth. To assure the accuracy of the dispersion relationship at such frequencies contained in the Gaussian pulse, this study used the phase-resolving linear mild-slope equations for propagating sinusoidal waves with various periods from Z_i to P_j. The Gaussian pulse was then represented as the linear sum of these sinusoidal waves. In the bathymetry data for computing the above-mentioned sinusoidal waves, the bed level of each grid was capped by a limit of 0.2 m below the still water level, even for the grid on the ground, so that computed water level fluctuations at the target point, P_j, were not affected by reflected wave components from the shore.

Finally, the aforementioned linear inversion was applied for primary and secondary wave components, respectively.

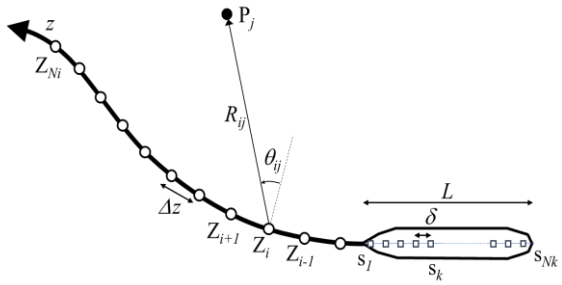

Figure 4 Schematic view of the present model

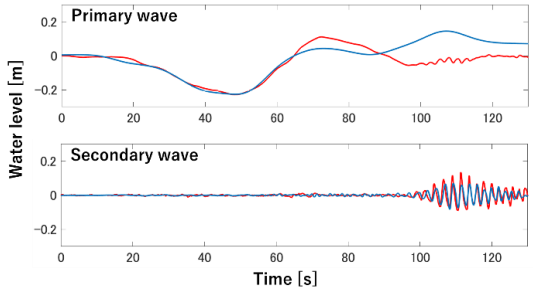

Figure 5 Observed and predicted water surface profiles of primary and secondary waves. Observation (red) and prediction (blue).

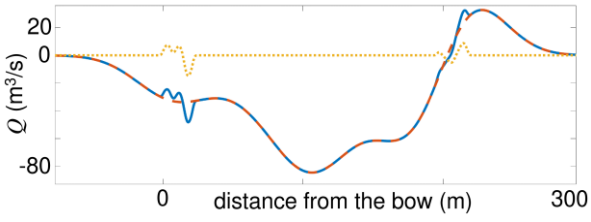

Figure 6 Estimated magnitude of Gaussian pulse (flow rate) for primary (red) and secondary (yellow) wave components and for both (blue).

To extract primary and secondary wave components, low-pass filter was applied to the observed water level fluctuations and the primary and secondary wave components were identified, as shown by the red lines in Fig. 5. Two Gaussian pulses with different widths were applied to prepare the Green's functions for each component.

RESULTS

Fig. 6 shows the distribution of the magnitude of the Gaussian pulse at each segment of the ship for representation of the primary and secondary wave components obtained through the linear inversion. In the model, the magnitude of the Gaussian pulse is determined as a flow rate, Q. As seen in the red dashed line, which indicates the magnitude of Gaussian pulse for the primary waves, negative values gradually vary over the entire ship body. This feature is reasonably consistent with the physical mechanism of the primary wave, i.e., a water level drop around the entire ship. The yellow dashed line indicates the magnitude of the Gaussian pulse for the secondary waves. Obtained fluctuations only around the bow and stern of the ship are also consistent with the physical mechanisms of secondary wave generation.

The blue lines in Fig. 5 show the water level fluctuations reproduced by the present model. As seen in the figure, the gap between observed and reproduced water level for the primary wave becomes larger after the first primary wave (t > 60 sec). This indicates that the observed data is affected by reflected wave component from the shore, whereas the model excluded the influence of reflected waves. In the comparison for the secondary waves, the reproduced waves tend to have milder crest profiles, indicating that the model is based on linear wave theory and does not capture non-linear wave effects.

DISCUSSIONS AND CONCLUSIONS

The present model reasonably well reproduced the observed water level fluctuations near the shore both for the primary and secondary wave components. As an example of model application, the obtained magnitude distribution of the Gaussian pulse shown in Fig. 6 can be used for determining the water level fluctuations along the offshore boundary of the arbitrary computation domain in which an appropriate wave model can compute more detailed wave propagation and deformation, including wave shoaling, breaking and reflections.

REFERENCES

Almström, Larson, Hallin (2022): Decision support tool to mitigate ship-induced erosion in non-uniform, sheltered coastal fairways, Ocean & Coast. Manag., 225, 106210.

Larson, Almström, Göransson, Hanson, Danielsson (2017): Sediment movement induced by ship-generated waves in restricted waterways, Coastal Dynamics 120.

Morioka, Tajima, Yamanaka, Larson, Kuriyama, Shimozono, Sato (2020): Numerical modeling of ship wave generation using Green's functions based on linear dispersive wave theory, Coast. Eng. J. Taylor & Francis, 62(2), pp.146-158.

Nwogu (1993): Alternative form of Boussinesq equations for nearshore wave propagation, J. of Waterway, Port, Coastal, and Ocean Eng., 119 (6): pp.618-638